^{77}Se Solid-State NMR of Inorganic and Organoselenium Systems: A Combined Experimental and Computational Study

John M. Griffin, Fergus R. Knight, Guoxiong Hua, Jeanette S. Ferrara, Simon W. L. Hogan,
J. Derek Woollins and Sharon E. Ashbrook

Supporting Information

S1. Further experimental details and centreband expansions for ^{77}Se solid-state NMR experiments

Table S1.1 summarises the number of coadded transients, recycle intervals and cross-polarisation contact times (where appropriate) used for recording the ^{77}Se solid-state NMR spectra shown in Figures 2, 4, 6 and 8.

Table S1.1 Experimental parameters for ^{77}Se solid-state NMR experiments performed for samples **1** – **17**.

Sample	Experiment	Magnetic field (T)	Number of transients	Recycle interval / s	Contact time / ms
1	MAS	14.1	32	300	-
1	Static	14.1	208	300	-
2	MAS	14.1	4	300	-
2	Static	14.1	12	300	-
3	MAS	14.1	4	240	-
3	Static	14.1	192	240	-
4	MAS	14.1	240	240	-
5	MAS	14.1	8	300	-
5	Static	14.1	4	300	-
6	CPMAS (5 kHz)	9.4	666	30	15.0
6	CPMAS (12.5 kHz)	9.4	1240	30	15.0
7	CPMAS	9.4	440	120	18.0
8	CPMAS	9.4	640	120	18.0
9	CPMAS	9.4	74	120	15.0
10	CPMAS	9.4	696	120	15.0
11	CPMAS	9.4	2598	120	18.0
12	CPMAS	9.4	656	120	18.0
13	CPMAS	9.4	102	120	15.0
14	CPMAS	9.4	492	120	15.0
15	CPMAS	9.4	474	120	15.0
16	CPMAS	9.4	114	120	15.0
17	CPMAS	9.4	694	120	10.0

The ^{77}Se static NMR spectra of samples **1** and **3**, and MAS NMR spectrum of sample **4** were recorded using a spin-echo pulse sequence (90°-τ-180°-τ-acquire) to remove baseline and lineshape distortions due to the short T_2 relaxation times. Spin-echo τ delays were 50 μs for **1**, 40 μs for **3**, and 71.4 μs for **4**.

^{77}Se static NMR spectra for samples **2** and **5** were recorded using the Carr-Purcell Meilboom-Gill (CPMG) pulse sequence[S1,S2] with an echo spacing of 500 μs. The number of echoes in the CPMG acquisition was 1000 for **2** and 1500 for **5**. The echoes were coadded prior to Fourier transformation.

Figure S1.1 shows expanded views of the isotropic resonances in the ^{77}Se CPMAS NMR spectra of compounds **7** - **17** shown in Figures 6 and 8.

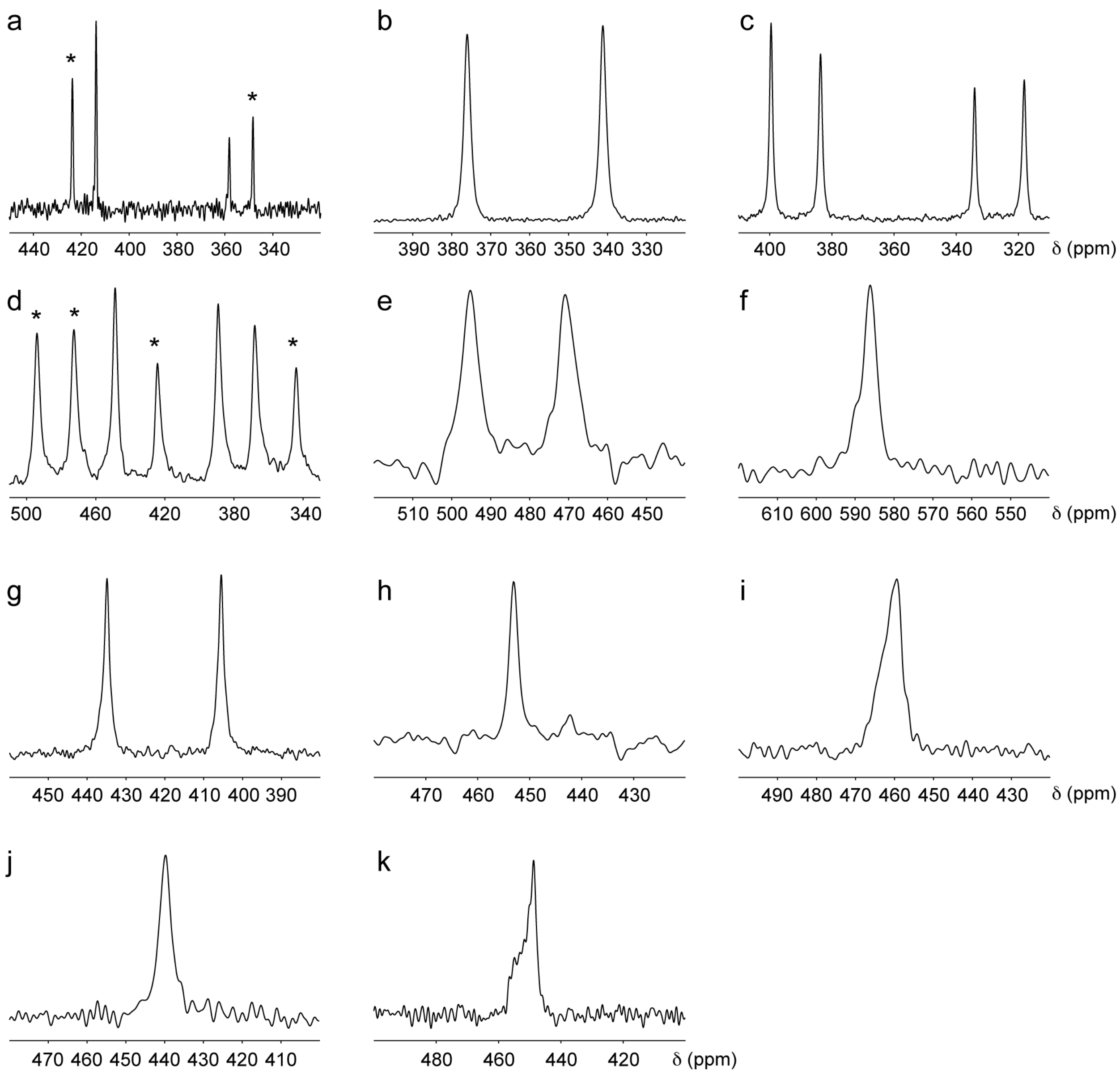

Figure S1.1. Expanded views of the isotropic resonances in ^{77}Se CP MAS NMR spectra of (a – k) compounds **7** – **17** shown in Figures 6 and 8.

S2. Powder X-ray diffraction data for SeO_2 (2)

In view of the apparent discrepancy between the ^{77}Se isotropic chemical shifts for **2** measured in this study and previous work,[S3] powder X-ray diffraction (PXRD) data was recorded to check the structure and purity of our sample. The experimental powder X-ray diffraction pattern for **2** is shown in Figure S2.1a. A simulated PXRD pattern based on the structure of McCullough *et al.*,[S4] shown in Figure S2.1b, shows good agreement with the experimental data. Additional lower intensity peaks can be attributed to the presence of small amounts of H_2SeO_3 (**1**) in the sample, which forms upon contact with moisture in the air. Indeed, a simulated PXRD pattern for **1** based on the structure of Larsen *et al.*,[S5] shown in Figure S2.1c, agrees well with the extra peaks observed in the experimental PXRD pattern. The presence of **1** does not explain the observed discrepancy between our ^{77}Se MAS NMR results and the previous study, as the isotropic resonance for **1** would be observed at 1288.1 ppm. For solid-state NMR experiments, a dried sample of SeO_2 was used.

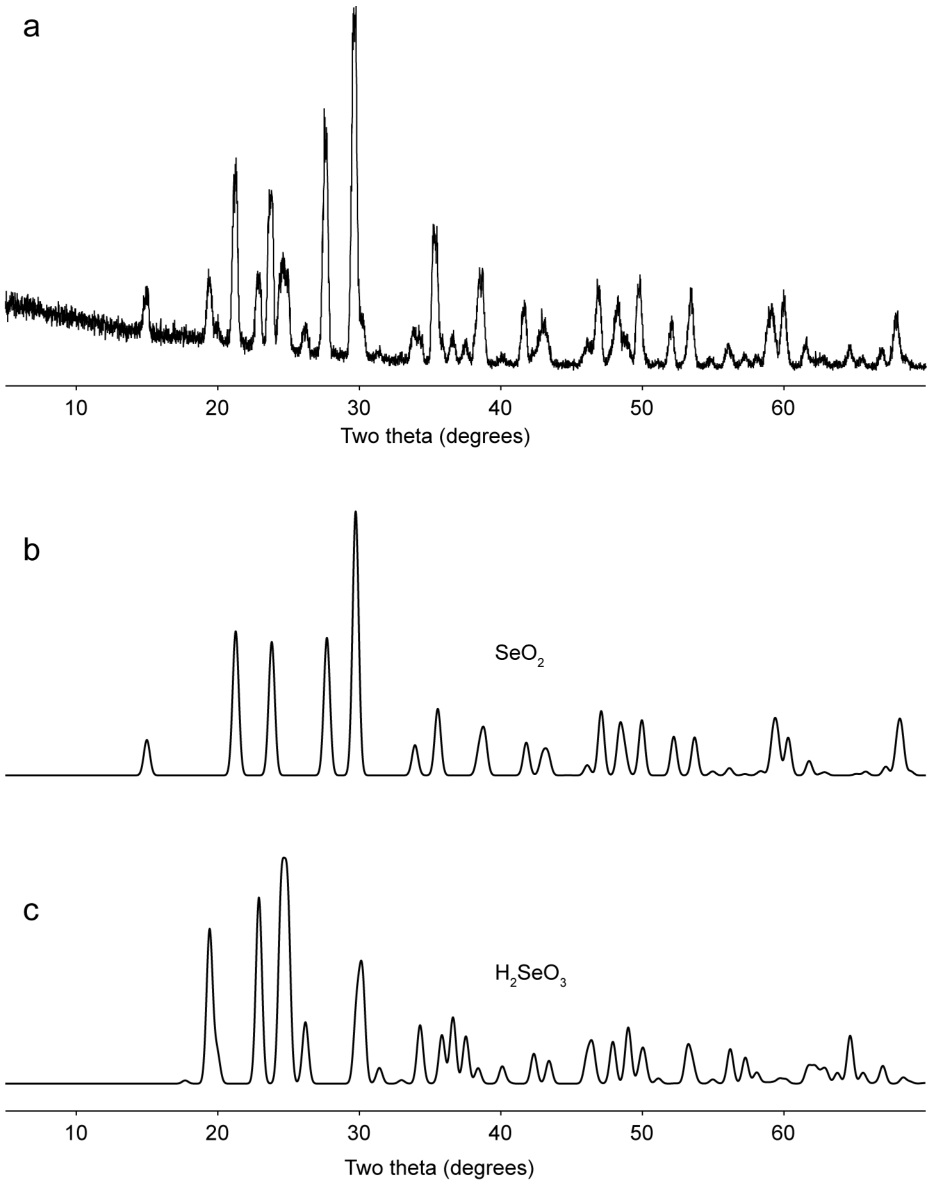

Figure S2.1. Experimental (a) and simulated (b) PXRD patterns for **2**. (c) Simulated PXRD pattern for H_2SeO_3 (**1**).

S3. ^{13}C CP MAS NMR spectra for compounds 6 – 17

^{13}C CP MAS NMR spectra for compounds **6** – **17** are shown in Figure S3.1. Spectra were recorded using Bruker Avance III spectrometers operating at magnetic field strengths of 9.4 T (samples **6**, **8**, **9**, **11** – **17**) and 14.1 T (samples **7** and **10**). All experiments were performed using a MAS frequency of 12.5 kHz with samples packed into 4-mm rotors, with the exception of **10**, which was packed into a 2.5-mm rotor. Chemical shifts are referenced relative to $(CH_3)_4Si$ at 0 ppm. All spectra were acquired using cross polarisation from ^{1}H, and ^{1}H TPPM decoupling during acquisition. The number of coadded transients, recycle intervals and cross-polarisation contact times used in each experiment are summarised in Table S3.1.

Table S3.1. Experimental parameters for ^{13}C CP MAS NMR experiments performed for samples **6** – **17**.

Sample	Magnetic field (T)	Number of transients	Recycle interval / s	Contact time / ms
6	9.4	600	120	1.0
7	14.1	342	60	1.5
8	9.4	112	120	1.0
9	9.4	1048	60	1.0
10	14.1	1000	5	1.0
11	9.4	56	120	1.0
12	9.4	56	120	1.0
13	9.4	32	120	1.5
14	9.4	68	120	1.5
15	9.4	572	120	1.5
16	9.4	152	120	1.5
17	9.4	362	20	1.5

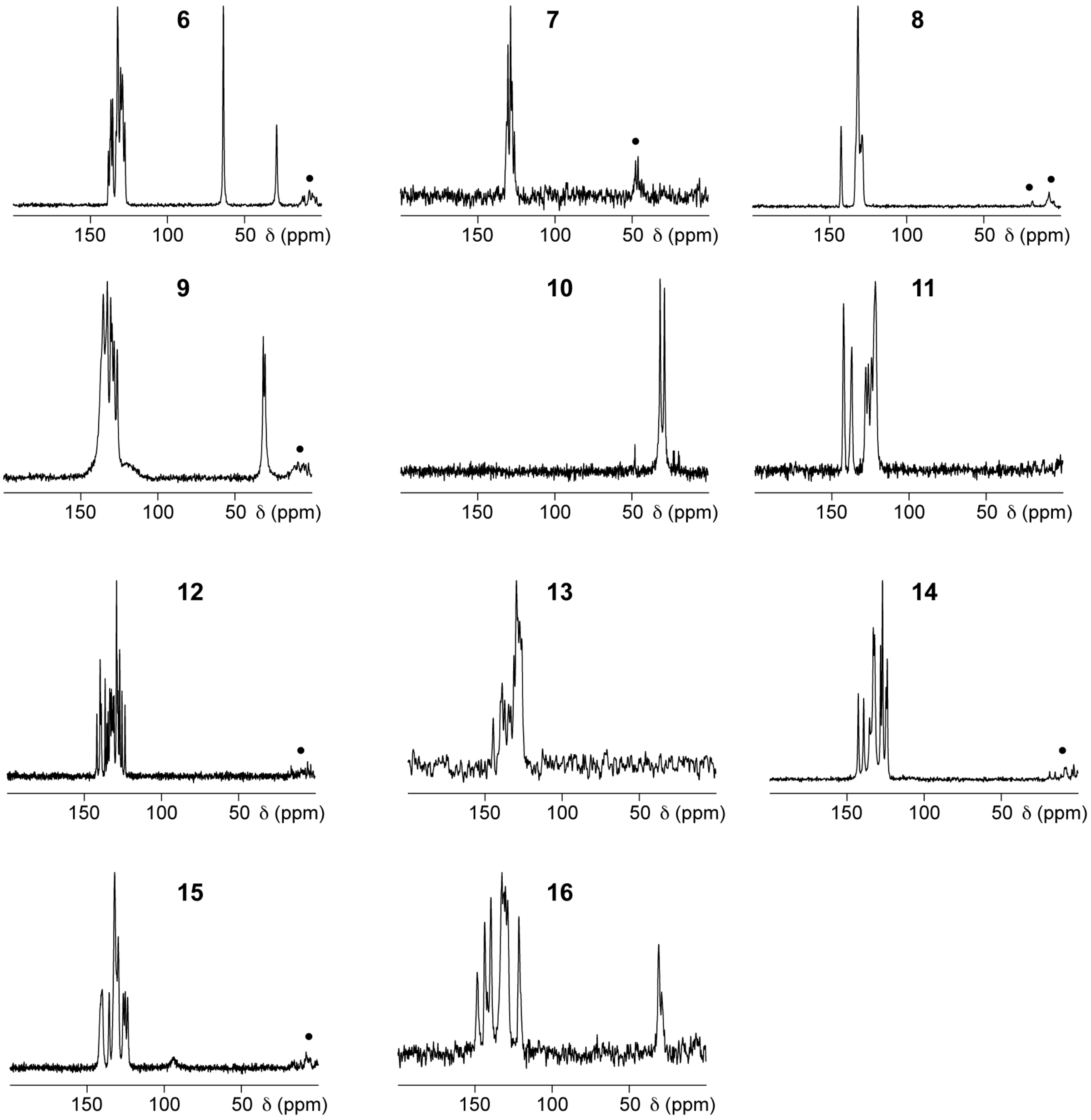

Figure S3.1. ^{13}C CP MAS NMR spectra for compounds **6** – **17**. Spinning sidebands or groups of spinning sidebands are indicated by black dots. Low intensity peaks observed in the spectra for **9**, **10** and **15** are attributed to residual solvent or impurity in the samples.

A plot of experimental ^{13}C chemical shifts against calculated chemical shieldings, shown in Figure S3.2, reveals a good correlation for most data points. However, data points corresponding to carbons in Se-C-Se environments (shown in purple) are found to lie significantly far from the line of best fit. Indeed, chemical shieldings for carbons with directly-bonded seleniums (shown in green) are found to be slightly less-well reproduced by the calculations in general. This suggests that the carbon chemical shift may be influenced by relativistic effects when directly bonded to the heavier selenium atom, and that this effect could be amplified for carbons bonded to two selenium species.

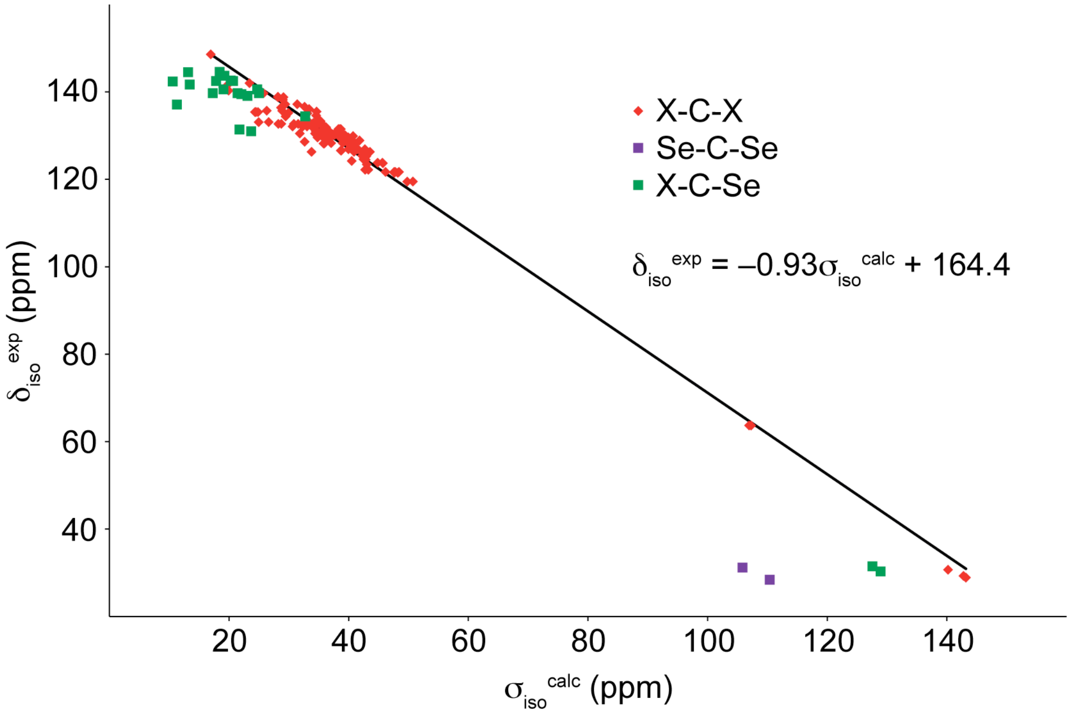

Figure S3.2. Plot of experimental ^{13}C chemical shifts, δ_{iso}^{exp}, against calculated isotropic chemical shieldings, σ_{iso}^{calc}, for compounds **1** - **17**. The solid line represents a linear fit to the data. Data points corresponding to carbons directly bonded to selenium atoms are shown in green. Purple data points correspond to carbons directly bonded to two selenium atoms.

S4. ^{31}P MAS NMR spectrum for 6

A ^{31}P MAS NMR experiment was performed on **6** using a Bruker Avance III spectrometer operating at a magnetic field strength of 9.4 T. The sample was packed into a 4-mm rotor and rotated at a MAS frequency of 8 kHz. The spectrum was acquired using cross polarisation from ^{1}H with a contact time of 1.5 ms, and ^{1}H TPPM decoupling during acquisition. The spectrum is the result of averaging 128 transients separated by a recycle interval of 10 s. ^{31}P chemical shifts are referenced to the isotropic resonance of BPO_4 at –29.4 ppm.

The crystal structure of **6**,[S6] shown in Figure S4.1a, contains two distinct P sites, P1 and P2. These are observed in the ^{31}P MAS NMR spectrum of **6**, shown in Figure S4.1a, at isotropic chemical shifts of δ_{iso}^{exp} = 66.4 and 64.6 ppm. From lineshape analysis of the spinning sideband patterns, it is possible to determine chemical shift tensor parameters for each site. These are summarised in Table S4.1. The experimentally determined values agree well with theoretical values obtained from the GIPAW calculations, summarised in Table S4.2. In an expanded view of the isotropic resonances, shown in Figure S4.1c, low intensity 'shoulders' are observed, corresponding to *J* couplings to the 7.6% abundant ^{77}Se. The magnitudes of the observed splittings are consistent with the values of 430 – 480 Hz and 810 – 830 Hz observed in the ^{77}Se CP MAS NMR spectrum of **6**.

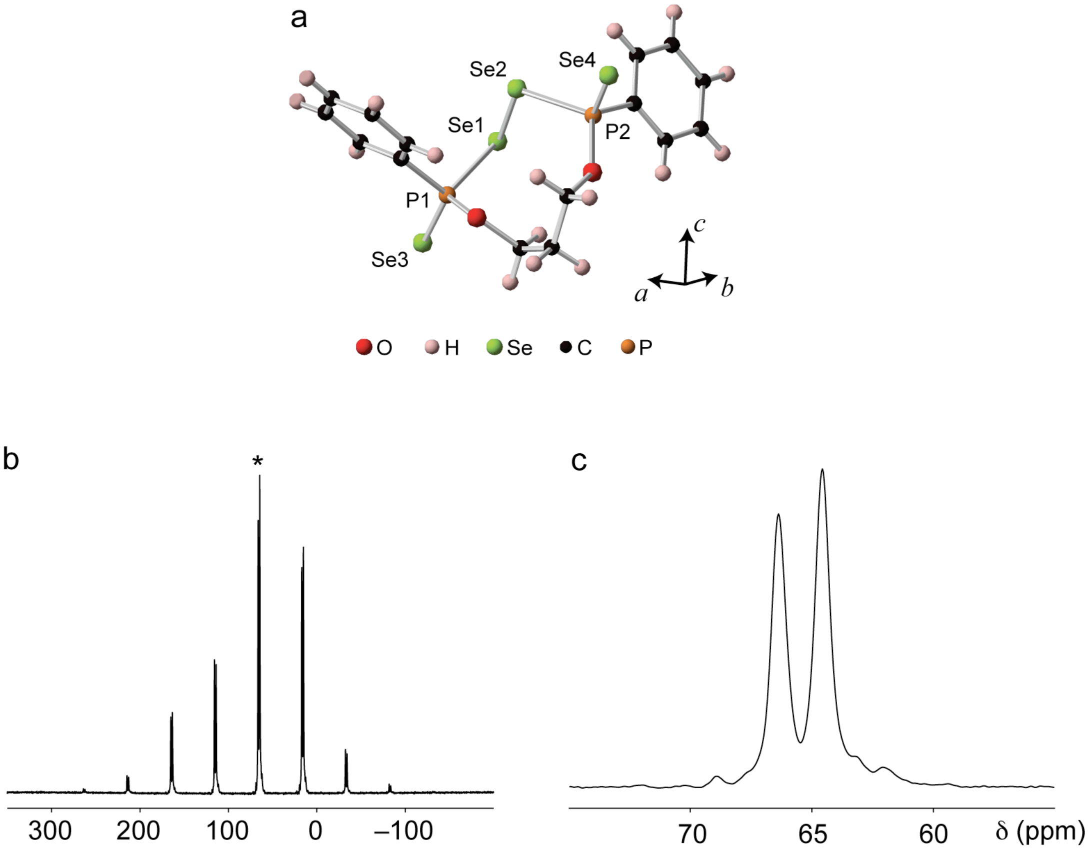

Figure S4.1. (a) Crystal structure of **6** showing the two distinct P sites. (b) ^{31}P CP MAS NMR spectrum of **6**. Isotropic resonances are indicated by an asterisk. (c) Expanded region of the ^{31}P CP MAS NMR spectrum shown in (b), showing the isotropic resonances and 'shoulders' resulting from *J* couplings to the directly-bonded, 7.6% abundant ^{77}Se.

Table S4.1. Experimental ^{31}P NMR parameters (isotropic chemical shift, δ_{iso}^{exp}, chemical shift tensor components, δ_{ii}^{exp}, and span, Ω_{CS}^{exp}) for compound **6**, extracted from the spectrum in Figure S4.1a.

Site	δ_{iso}^{exp}	δ_{11}^{exp}	δ_{22}^{exp}	δ_{33}^{exp}	Ω_{CS}^{exp}
P1	66.4(1)	195(2)	18(2)	–13(2)	208(3)
P2	64.6(1)	190(2)	20(2)	–16(2)	206(3)

All values are quoted in ppm.

Table S4.2. Calculated ^{31}P NMR parameters (isotropic chemical shift, δ_{iso}^{calc}, chemical shift tensor components, δ_{ii}^{calc}, and span, Ω_{CS}^{calc}) for compound **6**.

Site	δ_{iso}^{calc}	δ_{11}^{calc}	δ_{22}^{calc}	δ_{33}^{calc}	Ω_{CS}^{calc}
P1	66.1	188.3	48.1	–38.0	226.3
P2	65.3	191.2	54.0	–49.4	240.6

All values are quoted in ppm. Chemical shifts were determined from the calculated chemical shieldings using a reference shielding of 214.4 ppm.

S5. ^{27}Al NMR spectra of Al_2Se_3 (4)

For further insight into the structure of **4**, ^{27}Al solid-state NMR spectra were recorded. Experiments were performed using a Bruker Avance III spectrometer operating at a magnetic field strength of 14.1 T. The sample was packed into a 4-mm rotor and rotated at a MAS frequency of 14 kHz. Spectra are referenced relative to 1 M $Al(NO_3)_3$(aq).

The crystal structure of **4**,[S7] shown in Figure S5.1a, features two distinct Al sites, denoted Al1 and Al2. Both sites are tetrahedrally coordinated to four surrounding selenium atoms and have very similar local structural environments with respect to bond lengths and angles. As ^{27}Al (spin $I = 5/2$) is a quadrupolar nucleus, MAS NMR spectra are typically broadened by the second-order quadrupolar interaction, limiting resolution. A ^{27}Al MAS NMR spectrum shown in Figure S5.1b clearly shows a superposition of two second-order quadrupolar broadened lineshapes, from which quadrupolar and chemical shift parameters can be determined by a fit to the lineshape (shown in red). The second-order quadrupolar broadening can be removed using a two-dimensional multiple-quantum (MQ) MAS NMR experiment. A triple-quantum MAS NMR spectrum for **4**, is shown in Figure S5.1c. In this spectrum, the two resonances are clearly resolved in the isotropic dimension.

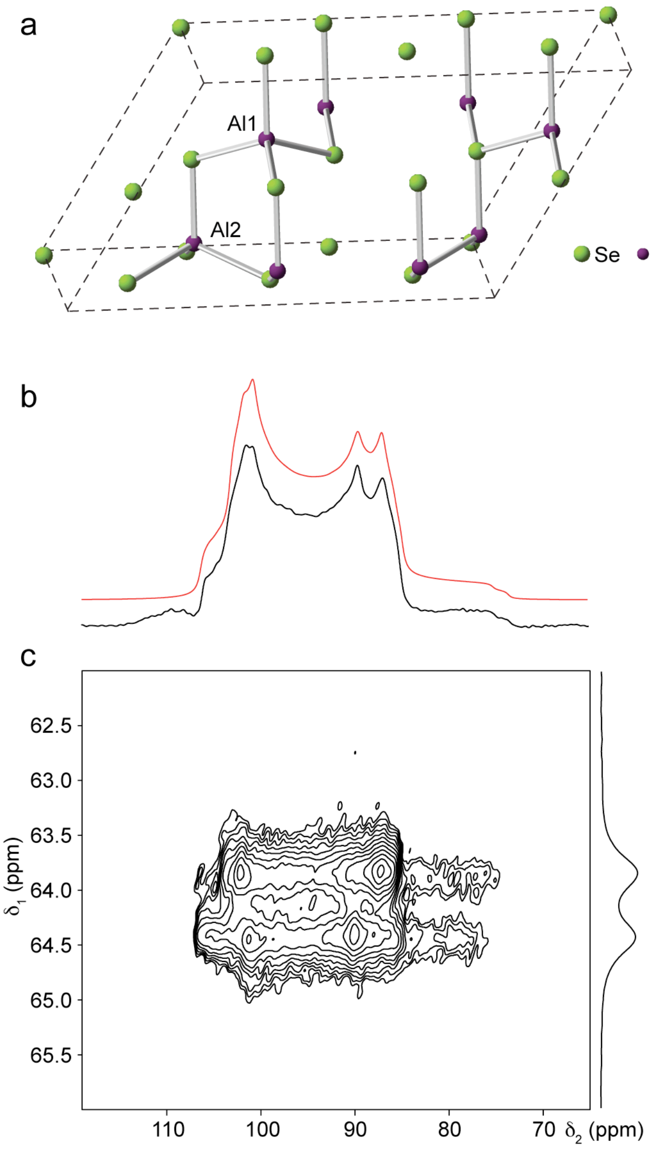

Figure S5.1. (a) Crystal structure of **4** showing the two crystallographically-distinct Al sites. (b) ^{27}Al MAS NMR spectrum of **4** (shown in black) and a fit to the experimental lineshape (shown in red). The MAS spectrum is the result of averaging 504 transients separated by a recycle interval of 3 s. (c) A two-dimensional triple-quantum MAS NMR spectra of **4**. The MQMAS spectrum was acquired using a phase-modulated split-t_1 shifted-echo pulse sequence and results from averaging 96 transients for each of 326 t_1 increments of 184.4 μs.

Table S5.1 compares the experimental values with calculated values obtained from the GIPAW DFT calculation on the optimised structure. Good agreement is observed between the calculated and experimental NMR parameters, with a slight underestimation of the C_Q for both sites.

Table S5.1. Experimental ^{27}Al NMR parameters (isotropic chemical shift, δ_{iso}^{exp}, quadrupolar coupling, C_Q, and asymmetry, η_Q) for compound **6**, extracted from the spectrum in Figure S5.1b.

	Experimental			Calculated		
Site	δ_{iso}^{exp} (ppm)	C_Q / MHz	η_Q	δ_{iso}^{calc} (ppm)†	$\lvert C_Q \rvert$ / MHz	η_Q
Al1	110.0(1)	7.49(1)	0.24(5)	109.75	6.82	0.29
Al2	107.6(1)	7.44(1)	0.13(5)	107.85	7.10	0.32

†Determined from the calculated chemical shieldings using a reference shielding of 511.75 ppm.

S6. References

S1. Carr, H. Y.; Purcell, E. M. *Phys. Rev.*, **1954**, *94*, 630.

S2. Meilboom, S.; Gill, D. *Rev. Sci. Instrum.*, **1958**, *29*, 688.

S3. Kemp, T. F.; Wong, A.; Smith, M. E.; Bishop, P. T.; Carthey, N. *Solid State Nucl. Magn. Reson.*, **2008**, *34*, 224.

S4. McCullough, J. D. *J. Am. Chem. Soc.*, **1937**, *59*, 789.

S5. Larsen, F. K.; Lehmann, M. S.; Søtofte, I. *Acta Chemica Scandinavica*, **1971**, *25*, 1233.

S6. Hua, G.; Li, Y.; Slawin, A. M. Z.; Woollins, J. D. *Angew. Chem. Int. Ed.*, **2008**, *47*, 2857.

S7. Steigmann, G. A.; Goodyear, J. *Acta Cryst.*, **1966**, *20*, 617.